UNIVERSITY OF AMSTERDAM

UvA-DARE (Digital Academic Repository)

Optically detected magnetic resonance and spin coherence in the phosphorescent state of exchange-coupled F+-center pairs in CaO

Gravesteijn, D.J.; Glasbeek, M.

DOI
10.1103/PhysRevB.19.5549

Publication date
1979

Published in
Physical Review. B, Condensed Matter

Link to publication

Citation for published version (APA):
Gravesteijn, D. J., & Glasbeek, M. (1979). Optically detected magnetic resonance and spin coherence in the phosphorescent state of exchange-coupled F+-center pairs in CaO. *Physical Review. B, Condensed Matter*, *19*(11), 5549-5558. https://doi.org/10.1103/PhysRevB.19.5549

General rights
It is not permitted to download or to forward/distribute the text or part of it without the consent of the author(s) and/or copyright holder(s), other than for strictly personal, individual use, unless the work is under an open content license (like Creative Commons).

Disclaimer/Complaints regulations
If you believe that digital publication of certain material infringes any of your rights or (privacy) interests, please let the Library know, stating your reasons. In case of a legitimate complaint, the Library will make the material inaccessible and/or remove it from the website. Please Ask the Library: https://uba.uva.nl/en/contact, or a letter to: Library of the University of Amsterdam, Secretariat, Singel 425, 1012 WP Amsterdam, The Netherlands. You will be contacted as soon as possible.

UvA-DARE is a service provided by the library of the University of Amsterdam (https://dare.uva.nl)

Download date:23 Aug 2022

Optically detected magnetic resonance and spin coherence in the phosphorescent state of exchange-coupled F^+-center pairs in CaO

D. J. Gravesteijn and M. Glasbeek
Laboratory for Physical Chemistry, University of Amsterdam, Nieuwe Prinsengracht 126, Amsterdam, The Netherlands
(Received 22 September 1978)

In yellow-colored CaO crystals a sharp zero-phonon line emission at 682.8 nm is observed. From optically-detected-magnetic-resonance experiments conducted at 1.3 K and at low- and high-magnetic-field strengths, it is concluded that the emission is due to a photo-excited triplet state of an orthorhombic *I* center. Optical polarization, spin alignment, and spin coherence decay phenomena were studied, the latter by means of techniques for the optical detection of spin echoes and spin locking, in order to determine the radiative and nonradiative properties of the triplet sublevels. The triplet state is associated with a $1s2p$ excited state of two electrons captured in two nearest-neighbor oxygen-anion vacancies (an F_2^{2+} center) with possibly a Ca^{2+} vacancy nearby for charge compensation (i.e., an F_2^{2+}-V^{2-} center). The observed linear dichroism in the excitation microwave double-resonance spectra is considered in connection with the mechanism for the triplet-state production. It is discussed briefly why the lowest $(1s)^2$ triplet state, which is predicted in the *M*-center model, could not be observed.

I. INTRODUCTION

The existence of exchange-coupled *F*-center pairs (*M* centers) in a number of different ionic crystals has aroused a great deal of experimental and theoretical interest.[1] Without exception, the *M*-type center has a singlet ground state and a low-lying triplet state (the energy separation being smaller than 0.7 eV), as expected for the analog of the hydrogen molecule in a crystal.[2] Especially observations involving this first excited triplet state (such a optically induced spin alignment[3,4] and magnetic field effects on the triplet lifetime[5]), have contributed in elucidating dominant processes in the optical pumping cycle.

In this paper evidence is presented for a new F^+-center pair in CaO that is remarkable because it possesses an excited triplet state which decays almost completely by phosphorescence in the *optical* region. It will be shown that the system is conveniently studied by means of optically detected magnetic resonance (ODMR) at either zero or high magnetic fields because of its favorable characteristics with respect to its fine-structure splittings, the (non-) radiative properties of the triplet sublevels, etc. The experimental data allow for a model of a nearest-neighbor pair of F^+ centers, lying along a ⟨110⟩ direction, in which the *second* excited state in the triplet ladder is responsible for the observed phosphorescence. Section II summarizes the experimental procedure. In Sec. III we present experimental results characteristic for the optical and magnetic properties of the emissive triplet state. It turns out that the *M* center provides an excellent example for the illustration of the feasibility of zero-field spin-coherence experiments on excited states in ionic solids. Finally, in Sec. IV the results are related to a model that correctly predicts the optical polarization and sign of the microwave-induced light changes under the condition of thermal isolation between the sublevels of the phosphorescent state.

II. EXPERIMENTAL

Yellow-colored CaO crystals were purchased from Spicer Ltd. The CaO crystal was mounted inside a slow-wave helix immersed in a He bath pumped down to 1.2 K. Optical excitation was by light from a 100-W high-pressure mercury PEK lamp filtered by an aqueous $NiSO_4$ solution or from a 500-W Xe Philips lamp in line with a Zeiss M20 grating monochromator. The phosphorescence emitted perpendicular to the exciting light was focused onto the entrance slit of a Hilger and Watts Monospek 1000 grating monochromator. For the photodetection an EMI GaAs photomultiplier was used. The zero- and low-field ODMR spectra were detected in the conventional way. Microwaves between 0.1 and 4 GHz were generated in a HP 8690B sweep oscillator unit outfitted with appropriate plug-ins. The microwaves were amplified up to 20 W by Varian traveling-wave-tube amplifiers and coupled to the helix by coaxial lines. Care was taken for optimum matching conditions. By switching positive-intrinsic-negative (*p-i-n*) diodes in the microwave circuit the microwaves could

 ©1979 The American Physical Society

be modulated ($\nu \sim 20$ Hz). At resonance, the synchronously induced modulation of the light changes was detected with a PAR lock-in amplifier. In high-magnetic-field experiments ($H \sim 3300$ G) for which an adapted Varian V-4500 EPR spectrometer was used, lock-in detection of the ODMR signal was possible by amplitude modulation of the external magnetic field.

The electronics necessary for the generation of the pulses in the coherence experiments were made of fast transistor-transistor logics; the microwave circuit is by and large similar to that described in Ref. 15. We will give a global description of the electronic equipment used for the coherence experiments. In the transient nutation experiments the *p-i-n* diodes were driven by a flip flop. The flip flop was set by means of the triggering pulse of a PAR lock-in amplifier. By using, for the reset pulse, the gate pulse of a PAR Model No. 162 boxcar averager, of which the delay time could be linearly swept, we were able to lengthen the microwave pulse duration proportional to the ramp of the boxcar averager. The pulses necessary for the optical detection of the electron-spin-echo decay were generated as follows. A pulse train from a crystal-driven oscillator with a frequency of 20 MHz was divided by means of the digital ramp of a Varian C-1024 time-averaging computer in such a way that the time between successive pulses is *proportional* to the ramp. The square pulses were fed into a counter. This counter selected a preset number of pulses (n) after it was triggered by the reference of the PAR lock-in amplifier. The counter released besides the preselected n pulses also an envelope pulse with overall width equal to the width of the pulse sequence. The two edges of the envelope pulse triggered $\frac{1}{2}\pi$ pulses in a monostable multivibrator, whereas the n-pulse train triggered n π pulses in another monostable multivibrator. Finally, the echo pulse sequence (with $n=1$ for a spin-echo- and $n>1$ for a Carr-Purcell-type experiment) was combined in an OR gate connected to the *p-i-n* diode driver.

In the echo and transient nutation type experiments, the microwaves were switched and fed into the traveling-wave-tube amplifier, and the resulting light changes were lock-in detected. Here we used the fact that just after the induced coherence the nonequilibrium population distribution, which is proportional to the coherence, decays radiatively in a time of the order of milliseconds, i.e., much longer than the characteristic times for the echo and transient nutation phenomena. Consequently the lock-in amplifier signal is proportional to the phosphorescence intensity at the end of the pulse sequence, provided that the repetition frequency is low enough (in our case less than 20 Hz). In the case of spin locking, the $\frac{1}{2}\pi$ pulses were as before generated from the envelope pulse. Now, however, the falling edge of the first $\frac{1}{2}\pi$ pulse and the trailing edge of the second were used to set and reset a flip flop connected to the *p-i-n* diode driver, resulting in a spin-locking pulse. The pulse circuit was adapted in order to avoid disturbing delays between the $\frac{1}{2}\pi$ pulses and the spin-locking pulse. Also, the microwave circuit had to be reorganized. The output of the microwave sweeper was separated into two channels by a hybrid "tee." The channels were 90° phase shifted with respect to each other and equalized in power. One channel was driven by the two $\frac{1}{2}\pi$ pulses, the other by the spin-locking pulse. The channel outputs were connected again by a hybrid "tee" after which the microwave power was amplified as described above. In case the spin-locking decay time was of the same order of magnitude as the radiative decay time, we could not use lock-in detection. Then we confined ourselves to real-time detection using the boxcar integrator.

III. RESULTS

A. Fine structure

On excitation of as-grown yellow-colored CaO crystals with blue light, emission spectra can be measured which are characterized by a sharp zero-phonon line (ZPL) at 5742 Å and an intense broad phonon sideband extending up to 700 nm.[6] As is well established, this emission is associated with the ${}^3T_{1u} \rightarrow {}^1A_{1g}$ transition in the CaO F center and has been the subject of detailed investigations in connection with Jahn-Teller coupling phenomena.[7–9] However, while detecting microwave-induced light changes in the broadband emission of the F center as a function of the microwave frequency, we found the ODMR response of two other defect centers. The first spectrum could be attributed to the excited triplet state in a F_A-Mo center as reported elsewhere.[10] The second spectrum comprises three transitions, two appeared in "normal" ODMR at 1.870 and 0.360 GHz, respectively [cf. Fig. 1(a)], and the third was found at 2.230 GHz in a triple-resonance experiment as described below. The phosphorescence-microwave-double-resonance[11] (PMDR) spectra obtained at either one of the three resonance frequencies, are as shown in Fig. 2. This spectrum is characterized by an intense, narrow ZPL at 682.8 nm and a broad, relatively weak, phonon sideband with bumps at 692 and 698 nm. The triplet nature of the state giving rise to the luminescence and microwave absorption could be established unambiguously from the orientation dependence of the ODMR spectra taken in the presence of an external magnetic field. For example, Figs. 3(a) and 3(b) show the splittings and shifts of the ODMR lines in two spectral regions, namely, 300–600 MHz

and 1.80–2.00 GHz, on rotating the crystal about a ⟨100⟩ direction perpendicular to the magnetic field $\vec{H}$ with H=64 G. Figure 4(b) shows representative ODMR spectra of the center taken with an EPR spectrometer operating at 9.15 GHz, with the experimental arrangement as depicted in Fig. 4(a), whereas Fig. 4(c) gives the angular dependence of these X–band spectra. No hyperfine structure could be resolved at any orientation of $\vec{H}$. All data, at low and high fields, could be fitted to the spin Hamiltonian of an S=1 system,

$$H=g\mu_B\vec{H}\cdot\vec{S}+D[S_z^2-\tfrac{1}{3}S(S+1)]+E(S_x^2-S_y^2) \quad (1)$$

with g=1.999±0.001, $|D|$=2049±1 MHz, and $|E|$=179±1MHz with $D/E>0$ (cf. Sec. III *b* and Fig. 5). The principal axes of the fine-structure tensor (x,y,z) were found, respectively, along the [110], [1$\bar{1}$0], and [001] axes of the CaO crystal. Thus we find that the center is of orthorhombic *I* symmetry[12] and in general gives rise to six magnetically inequivalent sites.

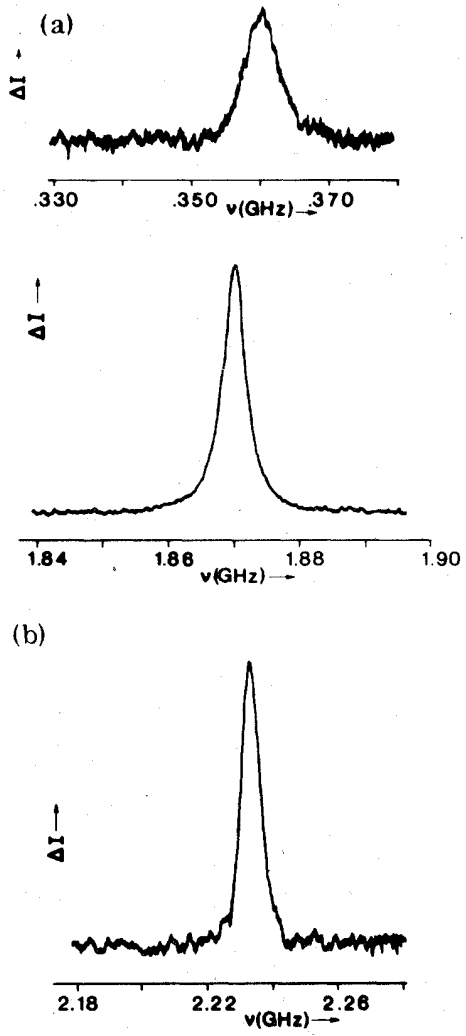

FIG. 1. Optically-detected-magnetic-resonance spectra in zero magnetic field of the M^{2+} center in CaO at a temperature of 1.3 K, detected at a wavelength of 682.8 nm. (a) The $2|E|$ transition is shown in the upper part, the $|D-E|$ transition in the lower part. (b) Optically detected ELDOR spectrum of the $|D+E|$ transition as obtained under continuous microwave pumping of the $|D-E|$ transition.

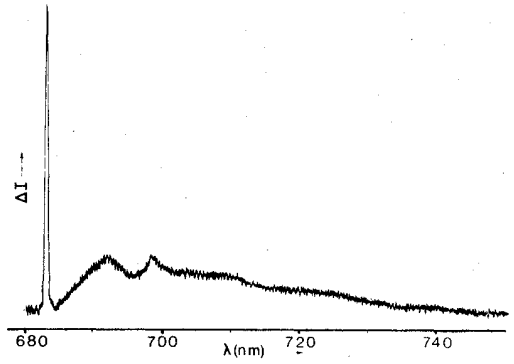

FIG. 2. Phosphorescence-microwave-double-resonance spectrum of the CaO M center in zero magnetic field at 1.3 K, taken with the microwave frequency at 1.870 GHz.

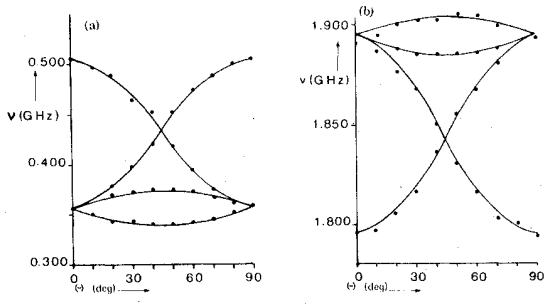

FIG. 3. Angular dependence of the ODMR transitions of Fig. 1(a), but now in the presence of an external magnetic field of 64 G, T=1.2 K. The crystal is rotated about a ⟨100⟩ axis. The dots in the figure refer to experimental values, the drawn lines show the calculated dependence for an orthorhombic *I* center with its *x*, *y*, and *z* axes along [110], [1$\bar{1}$0], and [001] directions, respectively, and fine-structure splittings D and E given by 2.049 and 0.179 GHz, respectively.

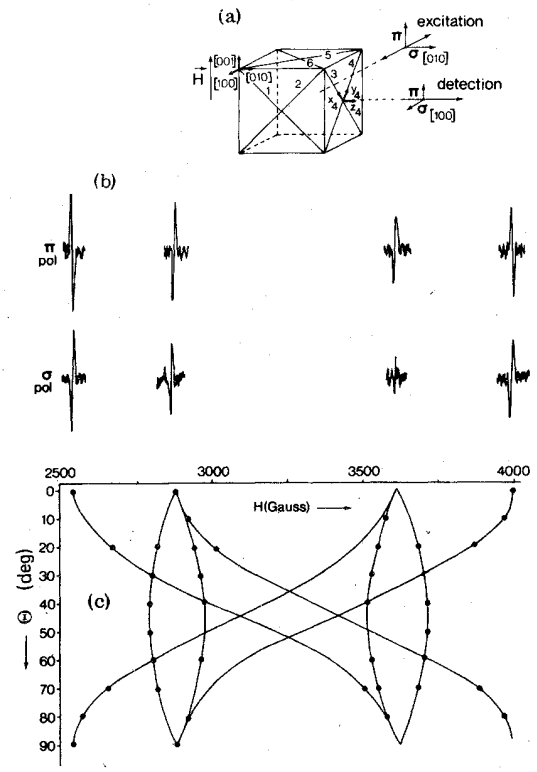

FIG. 4. Optically detected EPR spectra at X-band frequencies (ν=9.15 GHz). (a) Orientation of the main axes of the crystal with respect to the excitation and detection directions, the numbers along the face diagonals of the cube label the y axis of the different sites possible for the M center. (b) X-band ODMR spectra showing π- and $\sigma^{[100]}$-polarized light changes, respectively. The spectra were obtained with the experimental configurations as in (a). (c) Variation of the EPR line positions upon rotating the crystal about the [100] axis.

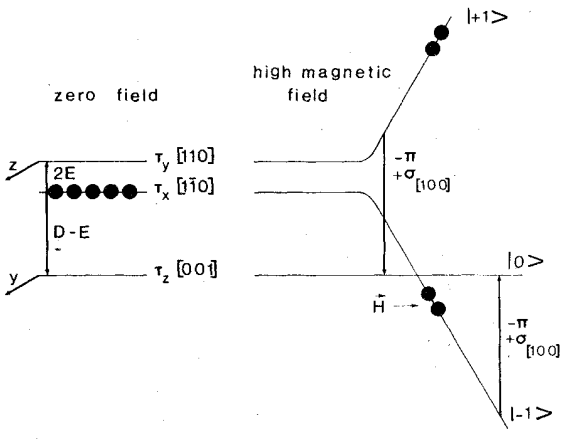

FIG. 5. Level scheme and emissive properties of the spin levels of the M-center triplet state as derived from experiments at, respectively, zero field and high magnetic fields (along the molecular z axis).

In zero-field ODMR the $|D+E|$ transition could not be observed directly. In order to circumvent the cause for the absence of the $|D+E|$ resonance (either the two spin levels involved in the $|D+E|$ transition are equally populated in the optical pumping cycle or these levels have the same radiative properties), we attempted an optically detected electron-electron double-resonance (ELDOR) experiment. Figure 1(b) shows the optically detected ELDOR spectrum with a maximum at 2.228 GHz. The spectrum is obtained from phase-sensitive detection of light changes at 683 nm induced by sweeping a modulated microwave frequency through resonance while continuously pumping the $|D-E|$ transition at 1.870 GHz. Note that all zero-field ODMR transitions, i.e., the $|D-E|$ and $2|E|$ in the double-resonance and the $|D+E|$ transition in the triple-resonance experiments, reflect a light increase at resonance. This result expresses a spin alignment in the triplet state which may be specified by a preferential occupation of a nonradiative spin level (τ_x), a far less effective occupation of the radiative levels (τ_y and τ_z), *and* a negligible spin-lattice relaxation during the triplet lifetime (3 msec). The spin isolation is also illustrated by observed level-anticrossing and cross-relaxation effects[13] on the phosphorescence intensity when a magnetic field is swept along a ⟨100⟩ crystal axis.

B. Optical polarization

In this subsection we will examine the selectivity in the photo-induced processes in more detail. Figure 4(b) shows the X-band ODMR spectra recorded for $\vec{H}$ parallel to a ⟨100⟩ crystal axis and with a linear polarizer in the detection pathway so that $\sigma_{[100]}$- and π-polarized light changes are detected separately [see also Fig. 4(a)]. In particular, we remark that for the (outer) Zeeman lines due to sites with their z axes along $\vec{H}$, the $\sigma_{[100]}$- and π-polarized light changes are opposite in sign (a $\sigma_{[100]}$-polarized light increase and a π-polarized light decrease). In the scheme of Fig. 5 we combine the results of (a) the zero-field and (b) the high-field optical-polarization measurements. The latter demonstrate that, in terms of the spin-axis frame of the center, the emission from the τ_y and τ_z levels are z and y polarized, respectively. These assignments are in agreement with the observed optical polarizations of the low-field Zeeman ODMR lines. For instance, for $\vec{H}$ and the exciting light along the [001] crystal axis, we find by detecting the intensity changes of light propagating along [010] at very low fields ($H < 30$ G) that the $|D-E|$ transition in sites with their z axes parallel to $\vec{H}$ is almost purely linearly polarized parallel to the [100] direction. This is as it should be since the $\tau_x \rightarrow \tau_z$ transition produces, according to Fig. 5, a light change which is y polarized in the molecular frame and therefore σ polarized in

the laboratory frame of which only the $\sigma_{[100]}$ component can be monitored when detection is along the [010] direction. As $\vec{H}$ is increased we expect τ_x to attain π-polarized radiative character because of mixing with τ_y. Thus, we anticipate a negative ratio of the π- and $\sigma_{[100]}$-polarized microwave-induced light changes at increasing magnetic field strengths. More precisely, if we adopt the polarization of the radiative levels to be as mentioned above, the ratio of the π- and σ-polarized light changes in the low-field experiment is calculated to vary as

$$\Delta I_{\pi_r}/\Delta I_{\sigma_r} = -(k_y^r/k_z^r)|E|[E^2+(g\mu_B H)^2]^{-1/2} \quad (2)$$

where k_y^r and k_z^r are the radiative decay rate constants for the y and z sublevels, respectively. As will be shown in Sec. III C, experimentally the rate constants for the *total* decay of the y and z sublevels can be determined, where it is understood that these rate constants (k_i^{exp}) comprise radiative (k_i^r) and nonradiative (k_i^{nr}) terms, $k_i^{exp}=k_i^r+k_i^{nr}$ with $i=y,z$. In Fig. 6 the drawn line is calculated from Eq. (2) based on the assumption that $k_i^{exp}=k_i^r$, whereas $k_y^{exp}=2.95\pm0.15$ msec and $k_z^{exp}=3.0\pm0.15$ msec as described in Sec. III C. The agreement between the calculated curve and the experimental points in Fig. 6 confirms that the decay of the y and z sublevels is radiative indeed.

Let us now focus on the processes in the excitation route. First, we show the excitation spectrum in Fig. 7 as detected from the ODMR intensity at 1.870 GHz as a function of the excitation wavelength. Selectivity in populating the spin levels was investigated in the following experiment. We used the experimental configuration given schematically in Fig. 8: excitation and magnetic field direction are along [001], detection is along the [1$\bar{1}$0] direction, whereas the polarization of the emitted light was measured either in the [110] or the [001] direction. This arrangement permitted us to study conclusively the excitation conditions for the defect center labeled 1 in Fig. 8, with x, y, and z axes along [1$\bar{1}$0], [110], and [001], respectively. This is seen as follows. We limit ourselves to sites with their z axes parallel to $\vec{H}$, labeled 1 and 2 in Fig. 8. For these centers the $|D-E|$ transitions are shifted to lower frequencies when a

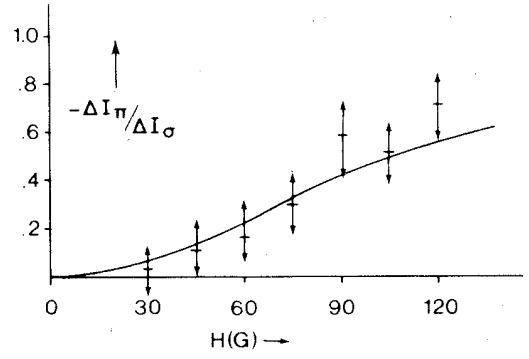

FIG. 6. Plot of the negative ratio of the π-polarized ODMR light changes and the $\sigma_{[100]}$-polarized ODMR light changes against the magnetic field strength as observed for the $|D-E|$ transition from sites with their z axes parallel to $\vec{H}$ as in the configuration of Fig. 4(a). Dots refer to experimental values, the drawn line shows the calculated dependence using Eq. (2) and $k_y^r=2.95$ msec and $k_z^r=3.0$ msec.

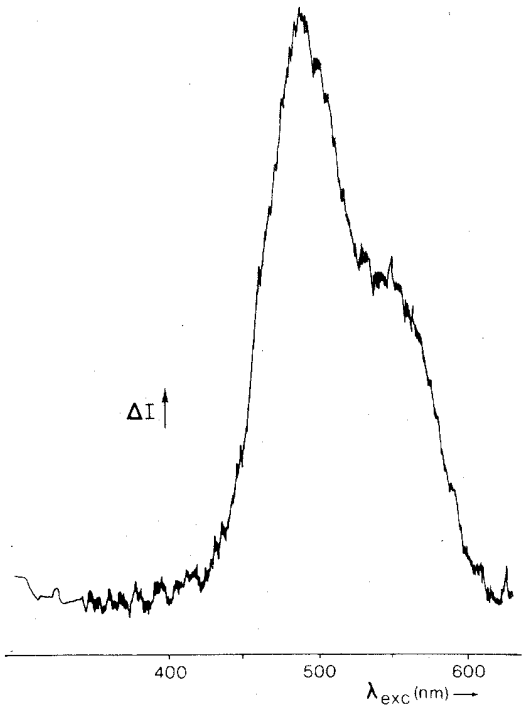

FIG. 7. Intensity of the zero-field ODMR transition at 1.870 GHz as a function of the excitation wavelength. The excitation source is a 500-W Xe lamp, the resolution of the excitation wavelength is 1.25 nm.

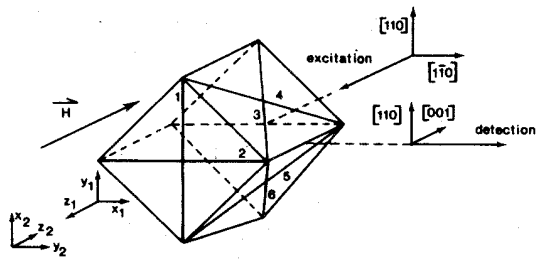

FIG. 8. Schematic representation of the directions in the experiment which studies selectively the ODMR response of site 1. The orientation of the molecular axes of centers 1 and 2 are as indicated, the face diagonals numbered 3–6 label the y axes of the other centers.

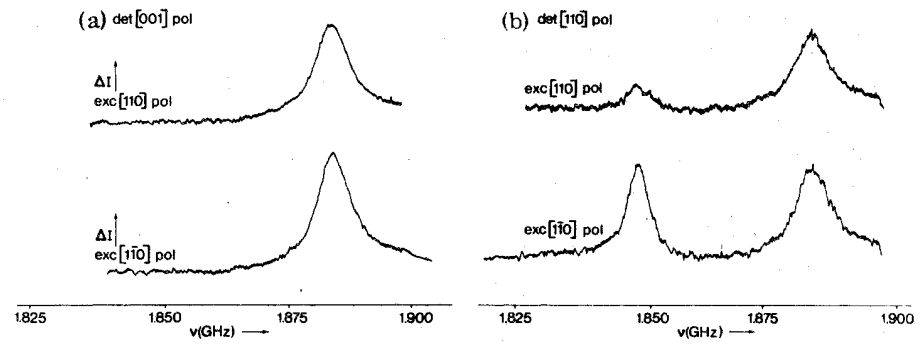

FIG. 9. Polarizations of low-field ODMR spectra ($H = 30$ G) as a function of the polarization of the exciting light when the configuration is that of Fig. 8. (a) Detection of the [001] polarized ODMR spectra when the excitation is polarized along the [110] or [1$\bar{1}$0] directions. (b) Detection of [110] polarized ODMR spectra when the excitation is polarized along the [110] and [1$\bar{1}$0] directions, respectively.

magnetic field of $H_{[001]} = 30$ G is applied. However, as explained above, for center 2 the shifted $|D-E|$ ODMR transition is y polarized in the center-spin-axis frame or [1$\bar{1}$0] polarized in the laboratory frame and therefore undetectable in the chosen experimental configuration. On the other hand, for center 1 only a [110]-polarized light increase is expected on microwave pumping the $\tau_x \rightarrow \tau_z$ transition in the presence of a small magnetic field. Figure 9 shows the ODMR spectra for the various polarizations of the pumping and detected light as indicated in the figure. Figure 9(a) shows that, on detection of [001]-polarized emission, only the signal from sites with their z axis oriented perpendicular to $\vec{H}$ is observed, but that the response of sites with their z axis collinear with $\vec{H}$ is absent, as expected. However, when [110]-polarized light changes are detected [Fig. 9(b)], we find that the shifted $|D-E|$ transition can be observed. Excitation with [1$\bar{1}$0]-polarized light (i.e., along the molecular x axis) yields then a somewhat stronger ODMR signal (I_x^{exc}) than with [110]-polarized light (along the molecular y axis); we find $I_x^{\text{exc}}:I_y^{\text{exc}} \simeq 5:3$, irrespective of the excitation wavelength. By a slight modification in the experimental configuration we determined $I_x^{\text{exc}}:I_z^{\text{exc}} \simeq 1:1$. In the latter case the crystal is rotated by 90° about the [1$\bar{1}$0] direction in Fig. 8, whereas the external magnetic field and the microwave field vector remained along the molecular z_1 and y_1 axes, respectively. Again, the linear dichroism is practically constant over the absorption band within, of course, the limit of the poor resolution of the excitation spectrum.

C. Spin coherence

When a microwave pulse resonant with the zero-field $|D-E|$ transition at 1.870 GHz is applied, we find a light increase which decays exponentially during the time interval the microwave power is turned off (see Fig. 10). The characteristic decay time is 2.95 ± 0.15 msec at 1.2 K. In a similar experiment on the $2|E|$ resonance, we found a decay time of 3.0 ± 0.2 msec. We note that the decay times are typical for excited triplet states in molecular and ionic solids for which the return to the singlet ground state is largely spin forbidden. Here it will be shown that the measured lifetimes correspond to the actual lifetimes of the *radiative* spin levels. This result is derived from microwave-induced coherence effects in the excited defect center. The technique is to couple electron spins coherently to a strong resonant microwave field of duration short compared with times associated with phase-destructive processes. If under such conditions a $\frac{1}{2}\pi$ pulse is applied, a nonvanishing magnetic moment oscillating at the resonance frequency is induced in the $S = 1$ spin ensemble expressing coherence. Recent investigations[14] have shown that many interesting details of dynamical processes as spin diffusion, decay to the electronic ground state, energy exchange to other localized and nonlocalized states, etc., can be studied by investigating the *loss* of phase coherence under a variety of external conditions. In the optical method[15] a final

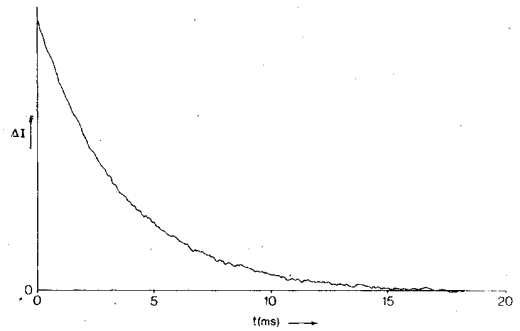

FIG. 10. Decay of the phosphorescence after a microwave pulse resonant with the $|D-E|$ transition at 1.2 K.

probe pulse is applied which transforms the residual coherence in the spin ensemble into triplet sublevel population changes that are measurable due to the distinctive radiative properties of the triplet sublevels. It was found in Sec. III B that an appreciable spin alignment can be achieved on photoexcitation of the defect triplet state, and also that the response of the individual spin levels can be studied selectively from optical-polarization properties. Thus, it would appear that techniques for optical detection of electron-spin coherence show great promise for investigating decay phenomena of the defect center indeed.

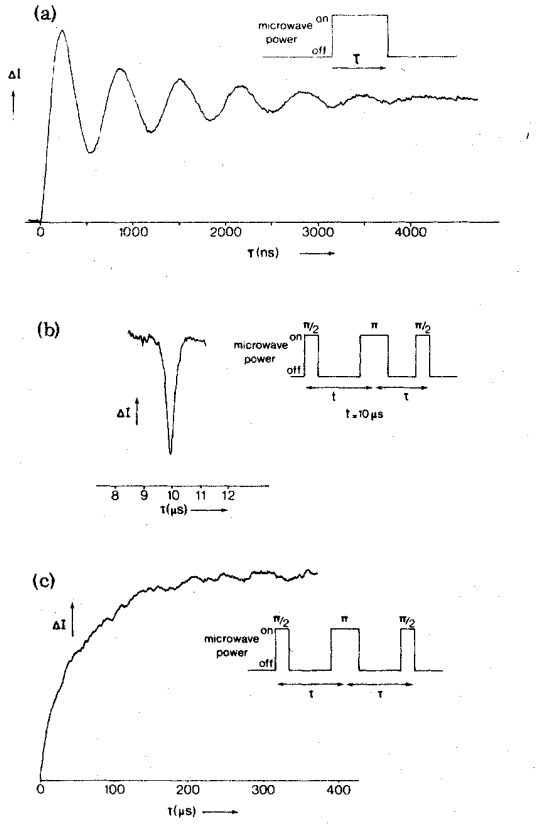

FIG. 11. Optically detected spin coherence phenomena at zero field in the phosphorescent triplet state of the CaO M center as monitored for the $|D-E|$ transition at 1.870 GHz, $T=1.2$ K. (a) Optically detected transient nutation; the phosphorescence intensity change is scanned as a function of the pulse length τ. (b) Optically detected spin echo; the pulse width of the $\frac{1}{2}\pi$ pulses is 100 nsec, the time between the first ($\frac{1}{2}\pi$) and the second (π) pulse is 10 μsec. The time between the second and third pulse is scanned (see also the inset). (c) Decay of the echo amplitude as a function of the time interval τ between two successive pulses in the pulse sequence (for the latter see the inset).

Coherent coupling of the spin system to a strong microwave field H_1 is demonstrated in a transient-nutation-type experiment.[16] Figure 11(a) shows the optically detected transient nutation as a function of the microwave pulse duration as detected for the $\tau_x \rightarrow \tau_z$ transition at 1.870 GHz at 1.2 K. From this coherent response the pulse length of $\frac{1}{2}\pi$ and π pulses necessary for an optically detected electron-spin echo could be determined. At zero field the ODMR echo experiment is characterized by a $\frac{1}{2}\pi$-τ-π-τ-$\frac{1}{2}\pi$ cycle of pulse events.[17] As in a conventional Hahn-echo experiment, in this case coherence is built up by the application of the π pulse which causes a rephasing of the spins that were initially dephased after the first $\frac{1}{2}\pi$ pulse, due to an inhomogeneous spread in local fields. The echo produced at 2τ is made optically detectable by the final $\frac{1}{2}\pi$ pulse. Figure 11(b) depicts an optically detected electron-spin echo at $\nu=1.870$ GHz, whereas Fig. 11(c) gives the decay of the echo amplitude as a function of the dephasing time τ. The latter decay is approximately exponential and characterized by a homogeneous dephasing time T_M with $T_M=140\pm10$ μsec at 1.2 K. However, in an optically detected spin-locking experiment at zero field[18] (the cycle of pulse events is now $\frac{1}{2}\pi$-90°- τ-90°-$\frac{1}{2}\pi$) the coherence decay time is lengthened to 5.0 ± 1.0 msec (cf. Fig. 12). In experiments of this type essentially the coherent-state *lifetime* is measured. The spins are locked to the microwave field vector because its amplitude is large in comparison with the local field fluctuations. In addition, as explained in Ref. 15, dephasing due to spin-spin interactions fluctuating randomly with time, and normally representing the spin diffusion effect on T_M, may now be suppressed (coherent averaging). The difference between the spin-locking decay time and T_M is attributed to this effect.

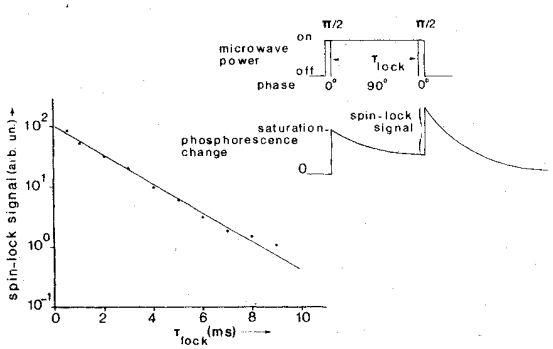

FIG. 12. Optically detected spin-locking decay at 1.870 GHz at 1.2 K. Plotted is the intensity change just after the second $\frac{1}{2}\pi$ pulse (see the inset) as a function of the spin-locking time τ. This change is detected with a boxcar averager.

The observed spin-locking decay time differs from that of the radiative τ_z level by a factor of 2. This can be understood when one realizes that the prepared superposition state is composed of equal parts of stationary τ_x and τ_z levels; apparently the coherence decay is governed by the decay of the radiative τ_z level whereas the contribution from the decay of the nonradiative τ_x level and all other dephasing processes are negligible. The measured lifetime of 2.95 ± 0.15 msec is therefore that of the τ_z level. As discussed in Sec. III B the decay for the τ_y and τ_z levels is predominantly radiative in character.

IV. DISCUSSION

The center discussed in this work is very likely an electron excess center, i.e., a defect containing electrons near anion vacancies. Alternatives for the origin of the observed phosphorescence like self-trapped excitons or trapped hole centers can be disregarded for a number of reasons. For example, a large Stokes shift is typical for self-trapped-exciton emission,[19] thus to produce the latter, ionizing radiation would be necessary for excitation. Also, apart from the special techniques often required for hole-center production, hole centers are annihilated relatively easily by optical or thermal means. None of these features were found for the defects investigated here. On the contrary, the defect was always present in CaO crystals containing F and F^+ centers and seemed to parallel these centers in stability against heat treatments in O_2 or H_2 atmospheres up to 1000 °C.

A CaO defect ZPL emission at 682.8 nm was reported previously by Gourley *et. al.*[20] These authors found that, on the application of a high magnetic field (7.7 T) or uniaxial stresses (up to 10 kg/mm^2), the defect ZPL emission splits in a manner qualitatively similar to that for the F center although the former splittings were of a much reduced magnitude. It was concluded that the defect and the F center should have similar local symmetry, the defect possibly being derived from H^-. On the other hand, the similarity with the optical absorption and the emission properties of the defect studied here is striking. In our case however, the high resolution of the ODMR experiments definitely excludes tetragonal point symmetry for the center. The orientation of the center-axis system with respect to the crystallographic main axes of the host crystal as determined in Sec. III A are pertinent to a stabilized F^+ dimer along a ⟨110⟩ crystal direction. Qualitative evidence is obtained from the measured fine-structure splitting D. On the assumption that the magnitude of D is completely determined by the magnetic dipolar interaction between the $S=\frac{1}{2}$ spins (remember also that the g value is close to 2), we find in the case of point dipoles,

$$D=-\tfrac{3}{2}(g\mu_B)^2/r^3 \ , \tag{3}$$

where r is the mean dipolar separation. For $D=2049$ MHz the calculated separation is 3.36 Å which may be compared with the nearest anion-pair separation in CaO along ⟨110⟩ of 3.39 Å. Thus, despite the restrictions in the approach, this result may, at least qualitatively, be considered as further support for a CaO M center.

Exchange-coupled F-center pairs in ionic solids have been discussed in a number of other studies.[1] In all cases neutral-charged pair centers were considered, e.g., in the CaO F_t center two electrons are trapped in the linear O^{2-}-Ca^{2+}-O^{2-} trivacancy and similarly, in the F_2 center in alkali halides, two electrons are located on two nearest-neighbor (nn) halogen-ion vacancies. The alkaline earth oxide analog would be four electrons trapped at two neighboring oxygen-anion vacancies. In a first approximation the situation would be that of a diatomic helium molecule (He_2) in a crystalline field; such a system is not expected to be stable. Hence, for the defect discussed here, we propose *two* electrons trapped at nn O^{2-} vacancies in the CaO lattice, this being an M^{2+} or F_2^{2+} center in the nomenclature of Sonder and Sibley.[21] As already noted, the center appears whenever F and F^+ centers are present which further indicates its general intrinsic nature. Unfortunately, our data are not definite about the existence of a nearby charge-compensating defect although it is tempting to assume that a neighboring Ca^{2+} vacancy along the [110] direction perpendicular to the F_2^{2+} axis acts as such.

As for the neutral M centers in alkali halides,[22] the energy-level scheme for the F_2^{2+}-V^{2-} center is most conveniently visualized in a simple Heitler-London approximation. Then the lowest excited state of the center is expected to be the $(1s)^2$ triplet state which transforms as $^3B_{3u}$ *or* $^3B_1$ in D_{2h} *or* C_{2v}, respectively. A rough semiempirical estimate of the splitting between this triplet state and the $(1s)^2$ singlet ground state using the method of Berezin[2] gives a value of 0.16 eV for the F_2^{2+} center in CaO. For an F_2^{2+}-V^{2-} center the splitting will probably be somewhat less because of the larger average distance between the electrons due to the effective negative charge brought about by the Ca^{2+} vacancy. In agreement with the expected order of magnitude for the exchange interaction, it appeared that no orthorhombic centers could be observed by EPR with a thermally accessible first excited triplet state.

The fact that the emission out of the triplet sublevels is purely linearly polarized is further support for the adopted defect structure. For $(F_2^{2+}$-$V^{2-})$-type centers the metastable, emissive triplet state is anticipated to belong to excited $(1s2p)$ configurations. In particular the observed optical polarizations (z for the τ_y level and y for the τ_z level) then correspond to

emission out of the $^3B_{3u}$ state ($^3B_1$ in C_{2v}), where it is assumed that the radiative character of the triplet sublevels is derived from admixing with appropriate singlet ($1s2p$) configurations.

The processes involved in the optical pumping sequence seem to be much less selective. The net dichroism in the excitation-microwave-double-resonance spectrum presents evidence that the triplet state is excited by intramolecular-intersystem-crossing (ISC) processes rather than indirect processes such as energy exchange or electron transfer as, e.g., do occur in M centers in KCl (Ref. 23) when the singlet is converted into a triplet. We do not find the linear dichroism to vary markedly over the excitation band despite the (weak) band structure (see Fig. 7). Thus, since the electric dipole moment involved in absorption is determined by the electronic orbital parts of the states that take part in the transition, we find that probably only one excited singlet state is involved in the ISC process to the emissive $^3B_1$ state. The mixed polarization of the absorption band is representative for vibronic mixing among the three electric-dipole-allowed $1s2p$ configurations in the *unrelaxed* excited singlet state. Because of this configuration mixing, ISC is, in principle, to all three spin states τ_x, τ_y, and τ_z. From the observed spin alignment (see Sec. III) one cannot conclude however, that the τ_x level is preferentially fed as compared with the τ_z and τ_y levels: spin selectivity in the decay must also be considered. The latter phenomenon turns out to contribute indeed since, as reported in Sec. III C, the decay of τ_x is negligible, whereas τ_y and τ_z were found to decay radiatively. The nonradiative decay components from either the τ_x, τ_y, and τ_z of the $^3B_1$ state were too small to be measured in the spin-coherence decay experiments and therefore are representative for a weak electron-lattice coupling in this state. This is also demonstrated by the low value of the Huang-Rhys factor S, $S = 2.35 \pm 0.15$, as determined from the intensity ratio of the ZPL and the whole band in the phosphorescence spectrum. This weak electron-lattice coupling is of significance as regards the possibility of feeding the predicted low-lying $1s^2(^3B_1)$ state by optical means: we find that excitation by what at first sight would seem to be the most probable route, namely, phonon cascade down from the next-higher photoexcited triplet state, is hampered by the extremely small electron-lattice coupling of the latter.

In summary, we have demonstrated that ODMR techniques enable us to detect explicitly the emission of the F_2^{2+} center in CaO at wavelengths where the emission due to other color centers is dominant. Experiments were designed to characterize further the distinct steps in the optical pumping cycle. From the observed optical polarization and spin-coherence decay phenomena we could identify in the energy-level scheme the $^3B_1$ state responsible for the phosphorescence at 683 nm. Excitation of the $^3B_1$ state is by means of ISC from a photoexcited vibronically mixed singlet state. Since in the techniques applied here the emissive triplet state is used as a probe, we inherently study only part of the full level scheme. This explains for the difference with the number of levels known for the F_2 center in alkali halides. An extension of the present work to other excited singlet and triplet states is in progress in order to obtain a more complete picture of the energy scheme. This would be important for a comparison of the possible photochemical properties of the F_2 center in CaO with those known for the M center in alkali halides.

ACKNOWLEDGMENT

The authors are grateful to J. H. Scheijde for skillful technical assistance in the spin-coherence experiments.

[1]For reviews see A. M. Stoneham, in *Theory of Defects in Solids* (Clarendon, Oxford, 1975); and B. Henderson and J. E. Wertz, in *Defects in the Alkaline Earth Oxides* (Taylor and Francis, London, 1977).

[2]A. A. Berezin, Phys. Status Solidi B 49, 51 (1972).

[3]D. H. Tanimoto, W. M. Zinniker, and J. C. Kemp, Phys. Rev. Lett. 14, 645 (1965).

[4]B. Henderson, J. Phys. C 9, 2185 (1976).

[5]J. M. Ortega, Phys. Rev. B 16, 3782 (1977).

[6]B. Henderson, S. E. Stokowski, and T. C. Ensign, Phys. Rev. 183, 826 (1969).

[7]P. Edel, C. Hennies, Y. Merle d'Aubigné, R. Romestain, and Y. Twarowski, Phys. Rev. Lett. 28, 1268 (1972); P. Edel, Y. Merle d'Aubigné, and R. Louat, J. Phys. Chem. Solids 35, 67 (1974).

[8]C. J. Krap, M. Glasbeek, J. D. W. van Voorst, Phys. Rev. B 17, 61 (1978).

[9]M. Glasbeek, J. D. W. van Voorst, Phys. Rev. B 17, 4895 (1978).

[10]D. J. Gravesteijn, J. H. Scheijde, and M. Glasbeek, Phys. Rev. Lett. 39, 105 (1977).

[11]D. S. Tinti, M. A. El Sayed, A. H. Maki, and C. B. Harris, Chem. Phys. Lett. 3, 343 (1969); C. B. Harris, M. Glasbeek, and E. B. Hensley, Phys. Rev. Lett. 33, 537 (1974).

[12]A. A. Kaplyanskii, Opt. Spectrosc. 16, 329 (1963).

[13]D. J. Gravesteijn and M. Glasbeek (unpublished).

[14]See, for example, W. G. Breiland, C. B. Harris, and A. Pines, Phys. Rev. Lett. 30, 158 (1973); J. Schmidt, Chem. Phys. Lett. 14, 411 (1972); C. A. van't Hoff and J.

Schmidt, *ibid.* 42, 73 (1976); M. D. Fayer and C. B. Harris, *ibid.* 25, 149 (1974).
[15]W. G. Breiland, H. C. Brenner, and C. B. Harris, J. Chem. Phys. 62, 3458 (1975).
[16]J. Schmidt, W. G. van Dorp, and J. H. van der Waals, Chem. Phys. Lett. 8, 345 (1971).
[17]W. G. Breiland, C. B. Harris, and A. Pines, Phys. Rev. Lett. 30, 158 (1973).
[18]C. B. Harris, R. L. Schlupp, and H. Schuch, Phys. Rev. Lett. 30, 1019 (1973).
[19]M. N. Kabler, Phys. Rev. 136, A1296 (1964).
[20]J. T. Gourley, W. A. Runciman, and E. R. Vance, J. Phys. C 8, 2329 (1975).
[21]E. Sonder and W. A. Sibley, in *Point Defects in Solids,* edited by J. H. Crawford and L. M. Slifkin (Plenum, New York, 1972), Vol. I, Chap. 4.
[22]H. Engström, Phys. Rev. B 11, 1689 (1975).
[23]I. Schneider and F. J. Keller, Phys. Status Solidi B 60, 175 (1973).